BILINGUAL PUBLISHING CO.
Pioneer of Global Academics Since 1984

Journal of Metallic Material Research
https://ojs.bilpublishing.com/index.php/jmmr

ARTICLE

Stereological Evaluation of Precipitates within Ferrite Grains in Heat-Treated 1.25Cr0.5Mo Steel Previously Exposed to Service

Rafael Fernández-Fuentes[1] Americo Scotti[2,4*] Amado Cruz-Crespo[1] Roberto Silva González[1] Rafael Ariza[2] Nelson Guedes de Alcantara[3]

1. Universidad Central Marta Abreu de Las Villas – UCLV, Cuba
2. Universidade Federal de Uberlândia – UFU, Brazil
3. Universidade Federal de São Carlos – UFSCar, Brazil
4. University of West, Department of Engineering Science, Trollhättan, Sweden

ARTICLE INFO

Article history
Received: 12 July 2019
Accepted: 30 September 2019
Published Online: 30 October 2019

Keywords:
Creep-resistant 1.25Cr0.5Mo Steel
Repairing
PWHT
Precipitation coarsening

ABSTRACT

The objective of this work was to study the effect of the heat treatment and further operation aging on the stereological parameters (size, quantity and volume fraction) of precipitates within ferrite grains of a creep-resistant 1.25Cr0.5Mo steel after long-term operation. The heat treatment was similar to the treatment that is carried out in industrial steam pipelines after welding (post weld heat treatment - PWHT) during installation and/or repairing. The operation aging corresponds to a subsequent long in-service operation after repairing. To determine the stereological parameters, SEM digital images were taken from samples of this material after conditions of in-service-aged (after long-term operation), in-service-aged and heat-treated (simulating repairing) and in-service-aged, heat-treated and in-laboratory aged (simulating subsequent long-term operation after repairing). The results indicate that the changes in the stereological parameters of the precipitates within ferrite grains after PWHT is associated with the coarsening process of the within-ferrite-grain precipitates as well as stabilizing the microstructure, since the material aging after PWHT of an in-serviced aged material would not change the stereological parameters.

1. Introduction

In electric power generation and oil processing plants, several structural steel components are subjected to working conditions that undergo mechanical loads at temperatures between 450 and 600 °C. This is the case of the steam generators and the respective pipelines used for steam conduction. Under these working conditions, these components experience the phenomenon known as creep, which can lead to failure due to plastic deformation over time and even breakage [1]. To ensure safe and long-term use of these components, low-alloy Cr-Mo steels have been developed, among other materials [2]. In these steels, the creep resistance is achieved by the action of two hardening mechanisms: solid solution and precipitation [3].

To uncover the creep resistance of the component material, accelerated tests are applied to determine the stress level at which a certain temperature causes the rupture or 1% of plastic deformation after 10^5 hours (11.4 years) by

**Corresponding Author:*
Americo Scotti,
Universidade Federal de Uberlândia – UFU, Brazil; University of West, Department of Engineering Science, Trollhättan, Sweden;
Email: americo.scotti@hv.se

Distributed under creative commons license 4.0 DOI: https://doi.org/10.30564/jmmr.v2i2.1017

means of the extrapolation. These accelerated tests use the Larson-Miller parameter (LMP), which represents the time and temperature equivalence for this type of steel under the thermally activated creep process of stress rupture. It permits the calculation of the equivalent times necessary for stress rupture to occur at different temperatures. [4]. However, in practice, it has been established that the useful life of the components manufactured with low alloy CrMo steel can reach and exceed 20 and even 30 years [5]. Nevertheless, premature failures frequently arise in the components manufactured with these steels that are associated with the weld region susceptible to the formation of non-acceptable cracks [6].

When these failures occur, and when it is technically-economically justified, repair is performed by removing the damaged section and welding an insert of a new material. The standards that are applied for this type of welding repair contemplate technological fabrication requirements to guarantee the quality of the welded joint of the new materials. However, the problem becomes complex in relation to the material exposed to service and which is thermally affected during the repair [7]. The complexity of the subject is increased when the application of post-weld heat treatment (PWHT) after repairing is required. In this regards, divergences in literature on whether PWHT after repairing is favorable or not from the point of view of the residual life, is noticed [7].

The PWHT is generally carried out in situ with localized heating, which imposes an additional thermal cycle on different regions of the weld (fusion – FZ - and heat-affected zones - HAZ) as well as the base metal that originally had not been exposed to the welding thermal cycle, as illustrated in Figure 1. Due to this localized heat treatment characteristic, it is not the whole component that undergoes the effect of the PWHT thermal cycle.

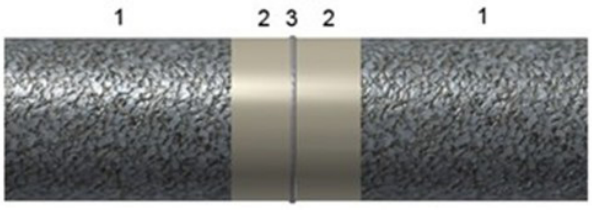

Figure 1. Schematization of the thermal affected zones associated with the localized (in situ) PWHT

Note: 1 - base metal not affected by the PWHT thermal cycle; 2 - zone of the base metal affected only by the PWHT thermal cycle; 3 - weld zone (fusion and HAZ) affected by both the welding and the PWHT thermal cycles.

The intrinsic complexity of the subject justifies the demand for further investigations on the effect of PWHT on the performance of creep-resistant low alloy CrMo steels. For example, knowledge about micro-structural stability, aiming at establishing how the microstructure behaves in steels subjected to creep, turns out to be of great importance to have elements for decision-making during maintenance of these industrial components. However, concurrent metallurgical phenomena lead to the variation of the microstructure under the effect of temperature and time. Consequently, attention has been paid to the relationship between microstructure and the behavior of steel under creep [8-11]. Among these phenomena, in the case of low alloy CrMo steels, spheroidization of perlite, graphitization, as well as precipitation, dissolution and growth of carbides stand out [12]. There has been a marked interest in studying the phenomena specifically related to the evolution of precipitates [2,13]. For this reason, the purpose of the present work is to study the influence of PWHT as part of a repairing procedure, just after repairing and after subsequent operation aging, on the stereological parameters (size, quantity and volume fraction) of precipitates within ferrite grains in 1.25Cr0.5Mo steel of a steam pipeline service-aged for more than 20 years at 480 ºC.

2. Materials and Methods

For this study, a 150-mm-long segment of the base material (with no weld) was taken from a pipe section that was removed (during repair operation) from a 300-mm-diameter and 12-mm-thick wall steam pipeline. This material had been in operation for approximately 20 years at 480 ºC. The determined chemical composition of the pipeline material (table 1) corresponds to that of an 1.25Cr0.5Mo steel, classified as A335 Grade P11, according to the ASTM A335 standard [14]. Using the material of this pipe segment, this work was carried out with samples under three experimental conditions (figure 2). The first one, referred hereafter as ISA (in-service-aged material, as removed from the pipeline, to be used as reference). A second condition (dedicated to evaluate the effect of a PWHT) referred to the same material of the ISA condition, but after undergoing a heat treatment to simulate the PWHT that is carried out after repair operations (hereafter referred as ISA+PWHT). Therefore, the ISA+PWHT condition is a simulation of the in-service-aged material (ISA condition) that would be affected only by the PWHT, i.e., a material corresponding to the region located between the weld affected zone and the base metal (section 2 of Figure 1). The heat treatment to simulate the PWHT was performed in a furnace, at a heating speed of 200 ºC h^{-1} and keeping a soaking time of 1.5 h at 700 ºC, in accordance with the recommendations of section VIII - division 1 of the ASME standard [15].

Distributed under creative commons license 4.0
DOI: https://doi.org/10.30564/jmmr.v2i2.1017

Table 1. Determined chemical composition of the pipeline material

C	Si	Mn	P	S	Cr	Mo	W	Ti	V
0.12	0.18	0.41	≤0.03	≤0.03	1.24	0.49	≤0.01	≤0.01	≤0.01

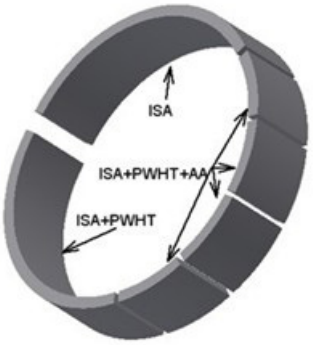

Figure 2. Sampling schematization of the pipe segment

Note: Corresponding to the studied experimental conditions, where ISA means the original material after in-service-aging, ISA+PWHT the original aged material to undergo heat treatment to simulate the PWHT and ISA+PWHT+AA the original aged and heat treated material to undergo accelerated thermal aging treatments.

Finally, a third condition (planned to evaluate the in-service thermal stability of the microstructure after the repair and PWHT) referred to the same material of the ISA+PWHT condition, but after undergoing accelerated thermal aging treatments (hereafter referred to as ISA+PWHT+AA). Four slices were removed for representing this latter condition (hereafter referred to as ISA+PWHT+AA-1, ISA+PWHT+AA-2, ISA+PWHT+AA-3 and ISA+PWHT+AA-4), aiming at different equivalent times during aging treatments. The aging parameters were selected so that they encompass ranges of temperature and time that would allow values of the Larson-Miller parameter (LMP) equivalent to times between 20000 and 100000 h at the service temperature (table 2). Therefore, the accelerated thermal aging treatments in this work was carried out using the same thermal cycle of a creep test, however without load application on the material.

Table 2. Time (t) and temperature (T) values for accelerated aging, Larson-Miller parameter (LMP) and equivalent time at the service temperature (teq).

Samples	T (°C)	t (h)	LMP=T(18 + log t)	t_{eq} (h)
ISA+PWHT+AA -1	550	1120	17325	101616
ISA+PWHT+AA -2	575	95	16830	22776
ISA+PWHT+AA -3	550	510	17042	42924
ISA+PWHT+AA -4	600	18	16810	21024

Specimens (10 mm x 10 mm x 10 mm) for Scanning Electron Microscopy (SEM) were taken from the steam pipeline material representing each experimental condition. They were prepared by grinding and polishing to a 1μm finish, according to ASTM E3-11 [16], and etching with 1 % NITAL, in accordance with ASTM E407-11 [17]. SEM digital images of 3072 x 2304 pixels and resolution of 10 nm/pixel were obtained. Using 10 images from each condition and a digital image processing software, micrograph processing was performed and the amount of precipitates per unit area (N_A) was counted. In addition, the equivalent 2D diameter (D_i), which depends on the area occupied by each section of precipitate in the image and on the volume fraction (V_V), according with the fraction of the area (A_A), were assessed.

From the particle sizes (D_i), the relative frequency histograms were made (using in all cases 15 classes of size equal to 0.04 μm and more than 2500 measured particles) and the probability density was determined in each class interval, which is calculated by dividing the number of counts for each size class of the observed distribution by the total number (N) of analyzed particles and the class width (ΔD) [18]. The experimental values of the probability density were adjusted to a lognormal probability density function with two parameters (equation 1) and the parameters of the distribution function were obtained according to [19]. So as to establish the quality of the adjustment, the coefficient of determination (c.o.d) and "test F" were used in the analysis of variance [20, 21].

$$f_{LN}(D_i;D_g,\sigma_g) = \frac{1}{D_i\sqrt{2\pi}\ln\sigma_g}\exp\left[-\frac{1}{2}\left(\frac{\ln(D_i/D_g)}{\ln\sigma_g}\right)^2\right] \quad (1)$$

where:

Di – equivalent 2D diameter, (μm)

D_g – geometric mean diameter, (μm)

σ_g – geometric standard deviation

From the 2D stereological parameters, the 3D parameters were determined: average diameter (D_V) and number of particles per unit volume (N_V), these two parameters are determined by the expressions (2) and (3) respectively [18]:

$$\overline{D_V} = \frac{\pi N}{2}\left[\sum_{i=1}^{N}\frac{1}{D_i}\right]^{-1} \quad (2)$$

$$N_V = \frac{N_A}{\overline{D_V}} \quad (3)$$

3. Results and Discussion

In the in-service aged material condition (ISA), the microstructure (figure 3(a)) is composed of ferrite-pearlite, in which the lamellar nature of the pearlite and the precipita-

Distributed under creative commons license 4.0 DOI: https://doi.org/10.30564/jmmr.v2i2.1017

tion inside the ferrite and in the grain boundaries are distinguished. This type of microstructure is common in low alloy Cr-Mo steels, yet Yang et al. [22] has observed this microstructure in 2.25Cr1Mo steel of steam pipelines exposed to long-term service. However, Afrouz et al. [23] reported the same microstructure in specimens from new steam pipelines subjected to creep test. In the in-service-aged material condition affected only by a simulated PWHT (condition ISA+PWHT), a microstructure (Figure 3(b)) qualitatively similar to the one from the ISA condition is observed, although some precipitates inside the ferrite are larger compared to those observed in the ISA condition.

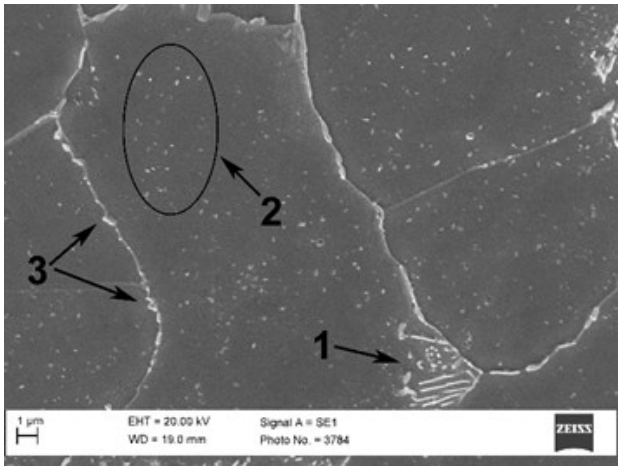

(a)

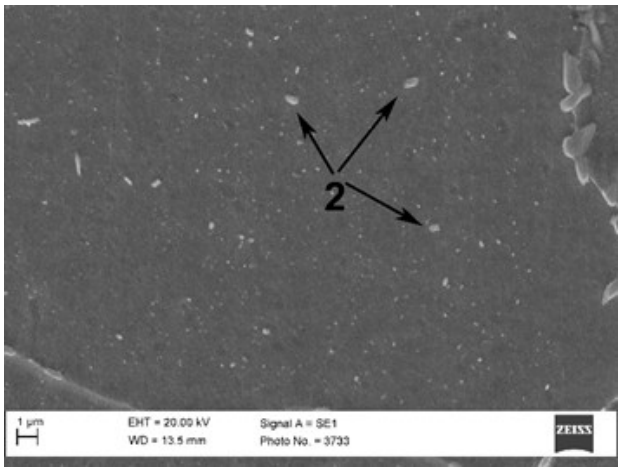

(b)

Figure 3. Representative SEM images of the material in the conditions

Note: (a) ISA; (b) ISA+PWHT, where: 1- lamellar pearlite; 2- within-ferrite-grain precipitates; and 3- grain boundary precipitates.

Taking now the samples from the third condition, i.e., in-service-aged material subjected to a heat treatment simulating a PWHT and also exposed to artificial aging conditions (ISA+PWHT+AA - n), a microstructure (Figure 4) qualitatively similar to those of the ISA and ISA+PWHT conditions is also observed, regardless the undergone aging treatment (table 2). According to these results, it can be inferred that neither the PWHT nor the thermal aging qualitatively modifies the type of microstructure of the material previously in-service (aged material): ferrite-pearlite with precipitation within ferrite grains and in the grain boundary, accompanied by lamellar pearlite

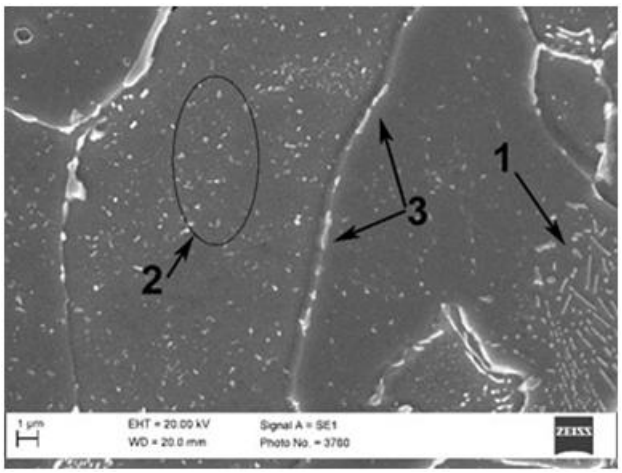

(a)

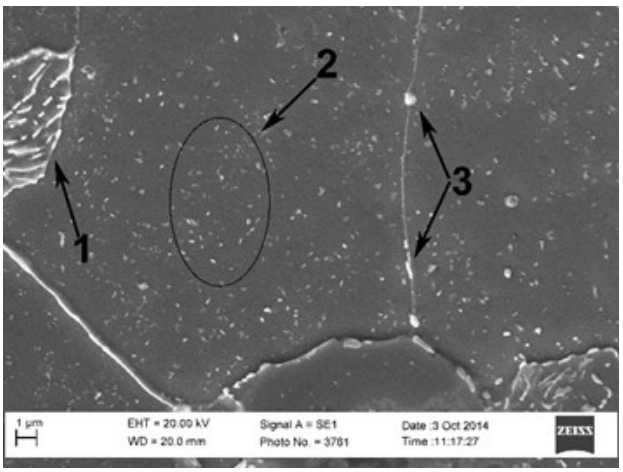

(b)

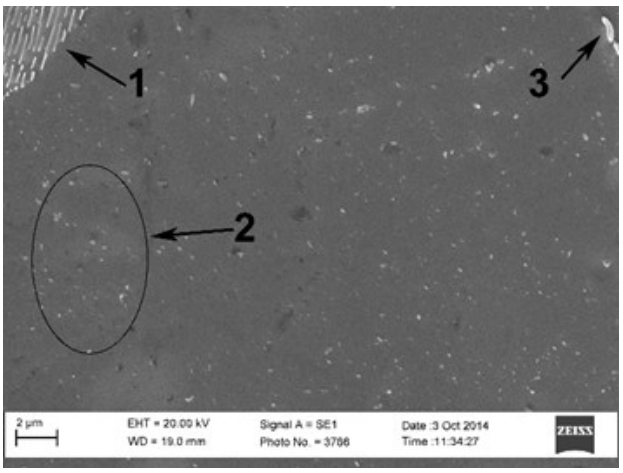

(c)

Distributed under creative commons license 4.0
DOI: https://doi.org/10.30564/jmmr.v2i2.1017

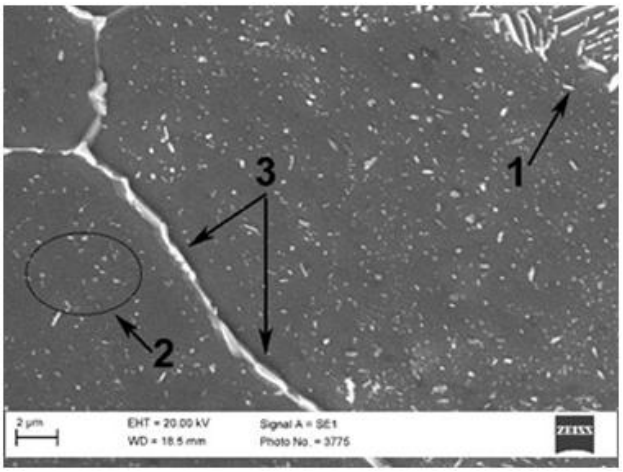

(d)

Figure 4. Representative SEM images of the material in the conditions (according to table 2)

Note: (a) ISA+PWHT+AA -1; (b) ISA+PWHT+AA -2; (c) ISA+PWHT+AA -3; and (d) ISA+PWHT+AA -4, where 1- lamellar pearlite, 2 – within-ferrite-grain precipitates and 3 – grain boundary precipitates.

The fact that the microstructures have not been modified qualitatively due to the effect of thermal aging does not mean that quantitative changes have not occurred, which are sometimes difficult to appreciate in SEM images. Among these changes, the variation of the type, size, quantity and volume fraction of precipitates within ferrite grains stands out. Regardless of whether there has been any change in the type of precipitates within ferrite grains or not, it is essential to know the other potential changes associated with them, since they intervene in the behavior of the mechanical resistance of the ferritic matrix (due to its precipitation hardening effect [24]), and because ferrite is the majority constituent of the alloy.

Figure 5 presents the relative frequency histograms and the particle probability density curves of the in-service-aged material condition (ISA) and the in-service-aged material after PWHT (ISA+PWHT). The particle probability density curves were raised by fitting curves to the experimental data, in which an adequate fitting to a lognormal probability density function is observed in both cases (c.o.d = 0.998 and p <0.001 for the ISA condition and c.o.d = 0.999 and p <0.001 for the ISA+PWHT condition).

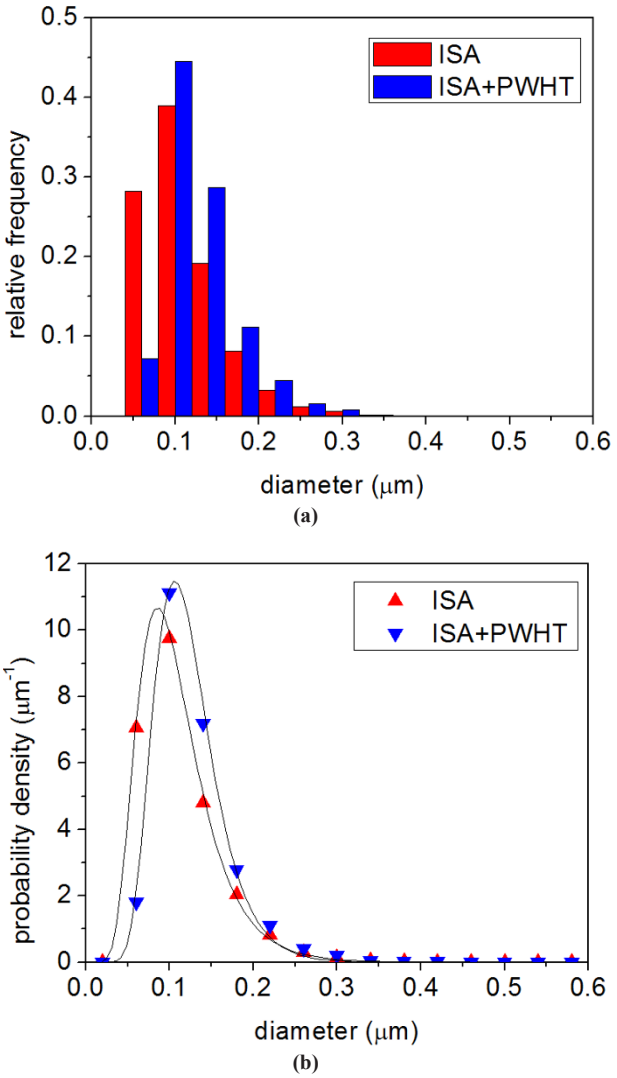

Figure 5. ISA and ISA+PWHT conditions: (a) - Relative frequency histograms of 2D size of within-ferrite-grain precipitates; (b) - particle probability density curves of the conditions

Based on the comparison of the histogram trends (figure 5 a), a quantitative effect of in-service PWHT on the 2D size distribution of within-ferrite-grain precipitates was evidenced. As seen, the relative frequency of the smaller class (0.04–0.08 µm) decreases considerably, while it increases at the remaining classes. In relation to the probability density function (figure 5 b), it is evident that the PWHT modifies the fitted curve, resulting in an increase of the mode (from 0.088 µm for the ISA condition to 0.105 µm for the ISA+PWHT condition), as well as the geometric mean diameter (from 0.101 µm for the ISA condition to 0.117 µm for the ISA+PWHT condition).

Figures 6 and 7, in turn, present similar charts of Figure 5 to compare the effect of ISA+PWHT and ISA+P-

Distributed under creative commons license 4.0 DOI: https://doi.org/10.30564/jmmr.v2i2.1017

WHT+AA conditions, the latter with different aging treatments, on the precipitate stereology. There were also adequate fittings to the lognormal type model for the different aging treatments (c.o.d equal to 0.994, 0.999, 0.992 and 0.998, respectively for the conditions ISA+PWHT+AA -1, ISA+PWHT+AA -2, ISA+PWHT+AA -3 and ISA+PWHT+AA -4, with $p < 0.001$ for all the cases). These results indicate that the thermal aging does not change the behavior observed in the ISA+PWHT condition, showing no significant variation of the relative frequency histogram of 2D size and the same particle probability density curves, keeping the value of the mode and the geometric mean diameter approximately equal under all conditions (0.1049 and 0.1170 μm, respectively).

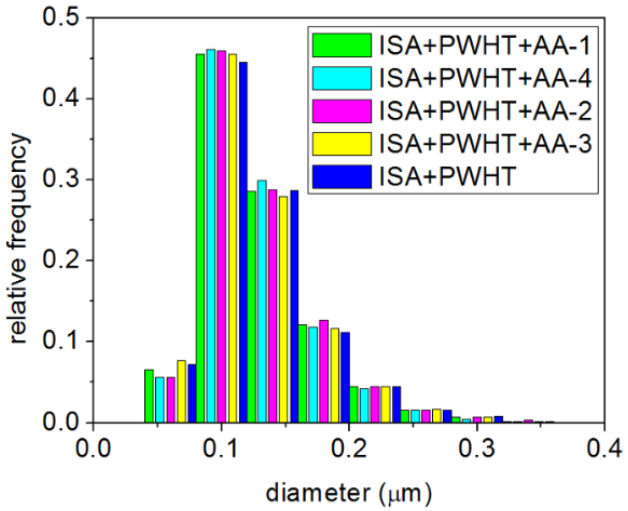

Figure 6. Relative frequency histograms of 2D size of within-ferrite-grain precipitates for the ISA+PWHT and ISA+PWHT+AA conditions, the latter as different aging treatments (according to table 2)

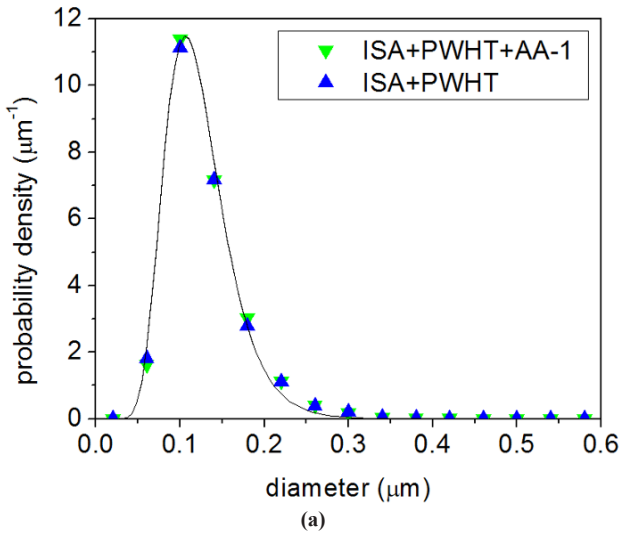

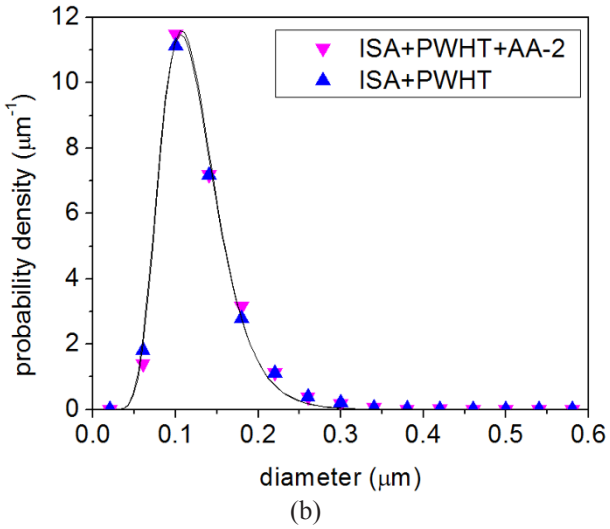

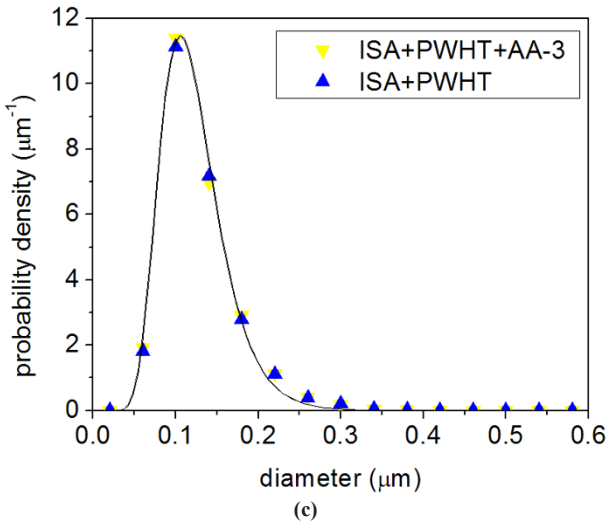

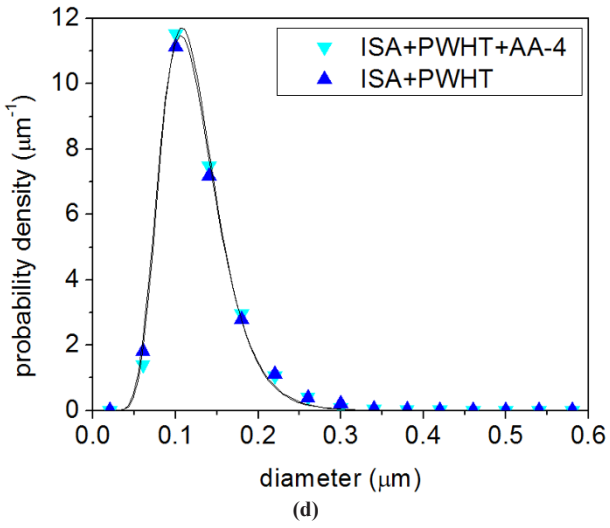

Figure 7. Particle probability density curves of the ISA+PWHT and ISA+PWHT+AA conditions, the latter at different aging treatments (according to table 2)

Distributed under creative commons license 4.0
DOI: https://doi.org/10.30564/jmmr.v2i2.1017

According to current literature [18,25], variations on the size distribution of precipitates can be associated with:

(1) precipitation of more stable particles: metastable precipitates that dissolve while nucleation and growth of more stable precipitates occurs (the amount of precipitates per unit volume is conserved and the average size and volume fraction are increased) or,

(2) coarsening processes: the growth of large precipitates at the expense of smaller ones which disappear (the volume fraction is conserved, the quantity of particles per unit volume decreases and the average size increases).

Therefore, and based on the stereological evaluation presented in Table 2, it can be stated that the coarsening process has been revealed in the present analysis, since there was an increase in the average size of the precipitates and decrease in their quantities per unit volume when the heat treatment to simulate the PWHT was applied on the long-term operation sample, yet keeping the values of the volume fraction similar. According to the results of Table 2, it can also be inferred that the PWHT stabilizes the precipitates within the ferrite grains, since the subsequent thermal aging treatments do not impose significative changes in the precipitates average sizes, in the quantities per unit of volume and the volume fractions.

Table 2. Within-ferrite-grain precipitate stereological parameters for the different material conditions

Condition	Stereological parameters		
	Mean Size 3D D_V (μm)	Quantity per unit of volume N_V (μm^{-3})	Volume fraction V_V (%)
ISA	0.147 ±0.015	70±8	3.1±0.5
ISA+PWHT	0.185±0.022	30±5	2.8±0.4
ISA+PWHT+AA -1	0.182±0.0183	33±3	2.6±0.4
ISA+PWHT+AA -2	0.186±0.022	31±4	2.3±0.5
ISA+PWHT+AA -3	0.183±0.020	28±4	3.0±0.5
ISA+PWHT+AA -4	0.188±0.023	31±3	2.2±0.4

5. Conclusions

The results of this work showed that the simulated PWHT applied over a sample of a 1.25Cr0.5Mo steel steam pipeline after service-aged for more than 20 years at 480 °C led to a coarsening process. Consequently, the precipitates within ferrite grains increased in size, from 0.147 ± 0.015 to 0.185 ± 0.022, counterbalanced by a decrease in the number of precipitates per volume unit (from 70 ± 8 to 30 ± 5), keeping the volumetric fraction. In addition, simulated post aging heat treatments of the samples which underwent a simulated PWHT showed to stabilize the within-ferrite-grain precipitates, with no further changes of their stereological parameters.

Acknowledgments

This work was supported by the bilateral agreement CAPES - Brazil / MES – Cuba (project number 146/12) and carried out at the Brazilian research laboratories LAPROSOLDA-LDTAD from Federal University of Uberlandia (UFU) and DEMa-CCDM from Federal University of Sao Carlos (UFSCar).

References

[1] E. Keim, D. Lidbury, Review of assessment methods used in nuclear plant life management, NULIFE Report. 2012, 12 (5): 70-81.

[2] G. Rigueira, H. Furtado, M. Lisboa, L. Almeida, Microstructural evolution and hardness changes in bainite and pearlite in Cr1Mo 2.25 steels after aging treatment. Revista Matéria, 2011, 16 (4): 857-867. DOI: 10.1590/S1517-70762011000400007

[3] F. Abe, Precipitate design for creep strengthening of 9% Cr tempered martensitic steel for ultra-supercritical power plants, Science and Technology of Advanced Materials, 2008, 9 (1): 1-15. DOI: 10.1088/1468-6996/9/1/013002

[4] F. Larson, J. Miller, A time-temperature relationship for rupture and creep stresses. Transactions of the ASME, 1952, 74: 765-775.

[5] H. Furtado, F. Santos, B. Cardoso, F. Matt, L. Henrique, Power plant remaining life evaluation. Key Engineering Materials, 2014, 588 (10-11): 232-242.

[6] K. Laha, S. Chandravathi, P. Parameswaran, S. Bhanu, S. Rao, L. Mannan, Type IV cracking in modified 9Cr-1Mo steel weld joint. Metallurgical and Materials Transactions A, 2007, 38 (1): 58-68. DOI: 10.1080/09603409.2015.1137158

[7] A. Fernández, N. Alcãntara, S. Haro, I. López, Effect of in service weld repair on the performance of CrMo steel steam pipelines. Materials Research, 2006, 9 (2): 153-158. DOI: 10.1590/S1516-14392006000200008

[8] G. Eggeler, Microstructural parameters for creep damage quantification. Acta Metallurgica et Materialia, 1991, 39 (2): 221-231. DOI: 10.1016/0956-7151(91)90270-B

[9] Y. Kadoya, E. Dyson, M. McLean, Microstructural stability during creep of Mo- or W-bearing 12Cr steels. Metallurgical and Materials Transactions A. 2002, 33 (8): 2549-2557. DOI: 10.1007/s11661-002-0375-z

[10] C. Lima, L. Pinto, L. de Almeida, Microstructural evolution of Cr-Mo ferritic steel (2,25Cr-1Mo) on

Distributed under creative commons license 4.0 DOI: https://doi.org/10.30564/jmmr.v2i2.1017

long term high temperature operation - precipitates fraction calculation. In: 5th Brazilian MRS Meeting. Florianópolis, Brazil, 2006.

[11] X. Yu, S. Babu, H. Terasaki, Y. Komizo, Y. Yamamoto, M. Santella, Correlation of precipitate stability to increased creep resistance of Cr–Mo steel welds. Acta Materialia, 2013, 61 (6): 2194-2206.
DOI: 10.1016/j.actamat.2012.12.040

[12] H. Furtado, I. Le May, High temperature degradation in power plants and refineries. Materials Research, 2004, 7 (1): 103-110.
DOI: 10.1590/S1516-14392004000100015

[13] C. Lima, L.Pinto, H. Furtado, L. de Almeida, M. de Souza, I. Le May, Quantitative observations of precipitation in 2.25Cr–1Mo steel exposed to different creep conditions in a power station. Engineering Failure Analysis, 2009, 16 (5): 1493-1500.
DOI: 10.1016/j.engfailanal.2008.09.009

[14] American Society for Testing and Materials. ASTM A335: Standard Specification for Seamless Ferritic Alloy-Steel Pipe for High-Temperature Service. ASTM International, West Conshohocken, PA, 2011.

[15] American Society of Mechanical Engineers. ASME Boiler and Pressure Vessel Code. Section VIII. Division 1. Rules for Construction of Pressure Vessels. ASME, 2010.

[16] American Society for Testing And Materials. ASTM E3-11: Standard Guide for Preparation of Metallographic Specimens, ASTM International, West Conshohocken, PA, 2011.

[17] American Society for Testing And Materials. ASTM E407-11: Standard Practice for Microetching Metals and Alloys, ASTM International, West Conshohocken, PA, 2011.

[18] P. Di Nunzio, H. Hougardi, Y. Lan, Modelling of particle growth and application to the carbide evolution in special steels for high temperature service. In: EUR 18633 — Properties and in-service performance. Luxembourg. 1999: 195.
ISBN: 9789282850442

[19] Y. Endo, Estimate of confidence intervals for geometric mean diameter and geometric standard deviation of lognormal size distribution. Powder Technology, 2009, 193 (2): 154-161.
DOI: doi.org/10.1016/j.powtec.2008.12.019

[20] R. Sultan, S. Ahmad, Comparison of parameters of lognormal distribution based on the classical and posterior estimates. Journal of Modern Applied Statistical Methods, 2013, 12(2): 304-313.
DOI: 10.22237/jmasm/1383279420

[21] K. Krishnamoorthy, T. Mathew, Inferences on the means of lognormal distributions using generalized p-values and generalized confidence intervals. Journal of Statistical Planning and Inference, 2003, 115 (1): 103-121 .
DOI: 10.1016/S0378-3758(02)00153-2

[22] J. Yang, Y. Huang, C. Yang, L. Horng, Microestructural examination of 2.25Cr1Mo steel pipes after extended service. Materials characterization, 1993, 30 (2): 75-88
DOI: 10.1016/1044-5803(93)90011-j

[23] A. Afrouz, J. Collins, R. Pilkington, Microestructural examination of 1Cr0,5Mo steel during creep. Metals Technology, 1983, 10(1): 461-463,
DOI: 10.1179/030716983803291569

[24] D. Baird, Strengthening mechanisms in ferritic creep resistant steels. In: Creep Strength in Steel and High Temperature Alloys. Proceedings... The Iron and Steel Institute, 1972: 207-216.

[25] D. Ouden Mathematical Modelling of Nucleating and Growing Precipitates: Distributions and Interfaces. Dissertation at Delft University of Technology. Netherlands, 2015.

Distributed under creative commons license 4.0
DOI: https://doi.org/10.30564/jmmr.v2i2.1017